crystals

MDPI

Article

Long Rod-Like Liquid Crystal Containing Azobenzene and the Applications in Phase-Transition Regulation and Orientation of Nematic Liquid Crystal

Qing Wang, Huang Chen, Hao Xing, Yuan Deng, Zhi-Wang Luo and He-Lou Xie *

Key Lab of Environment-Friendly Chemistry and Application in Ministry of Education, and Key Laboratory of Advanced Functional Polymer Materials of Colleges, Universities of Hunan Province and College of Chemistry, Xiangtan University, Xiangtan 411105, China; 201921001553@smail.xtu.edu.cn (Q.W.); 201510141360@smail.xtu.edu.cn (H.C.); 202021001879@smail.xtu.edu.cn (H.X.); 201821531564@smail.xtu.edu.cn (Y.D.); 202031000166@smail.xtu.edu.cn (Z.-W.L.)
* Correspondence: He-lou@xtu.edu.cn

Abstract: Phase-transition and orientation of liquid crystal (LC) are two crucial factors for LC application. In this work, a long rod-like LC compound containing double azobenzene (M1) is successfully designed and synthesized. The combing technologies of nuclear magnetic resonance (^{1}H NMR, ^{13}C NMR) and Fourier transform infrared spectroscopy (FTIR) are used to identify the chemical structure of the molecule. Additionally, the polarized optical microscopy (POM), differential scanning calorimetry (DSC), and one-dimensional wide-angle X-ray diffraction (1D WAXD) experimental results show that M1 exhibits an ultrawide range of LC phases and a stable LC structure even at ultrahigh temperature, which indicates that this LC can be applied in some especial devices. Further, the compound M1 is used to tune the LC temperature range of the commercial LC 4-cyano-4′-pentylbiphenyl (5CB). A series of samples 1–7 are obtained through doping different contents of M1, which show different LC temperature ranges that are dependent on the composition ratio of M1 and 5CB. More interestingly, all resultant samples show spontaneous vertical orientation on the hydrophilic glass substrate. Meanwhile, due to the effect of azobenzene in the compound M1, a reversible transition between homeotropic to random orientation of the LC molecules is achieved when these LC cells are alternately exposed to UV irradiation and visible light, which implies that this material shows potential application in especial display and optical storage technologies.

Keywords: phase-transition regulation; LC orientation; azobenzene LC

Citation: Wang, Q.; Chen, H.; Xing, H.; Deng, Y.; Luo, Z.-W.; Xie, H.-L. Long Rod-Like Liquid Crystal Containing Azobenzene and the Applications in Phase-Transition Regulation and Orientation of Nematic Liquid Crystal. *Crystals* **2021**, *11*, 418. https://doi.org/10.3390/cryst11040418

Academic Editors: Jose Adrian Martinez-Gonzalez, Xiao Li and Camille Bishop

Received: 14 March 2021
Accepted: 9 April 2021
Published: 13 April 2021

1. Introduction

Liquid crystal (LC), as the most common and important material in modern society, shows tremendous applications in displays, optical devices, sensors, information storage, transmission, and so on [1–6]. The LC performance is significantly dependent on the molecular structure, phase transitions, and phase structures [7–10]. In order to obtain LC materials with excellent performance, tremendous LCs with different molecular structures have been successfully designed and synthesized, such as rod-like LC, dish-like LC, bowl-like LC, ball-like LC, and amphipathic LC [11–15]. Meanwhile, the relationship between structure and property has been explored for practical applications and academic interests. Numerous experimental results and practical applications have indicated that the rod-like LC molecules with nematic phase show excellent performance in modern display technologies [16–18]. For example, the commercial LC molecules such as 4-cyano-4′-pentylbiphenyl (5CB) [19], 4-cyano-4′-heptylbiphenyl (7CB) [20], 4-cyano-4′-octanoylbiphenyl (8OCB) [21], and 4-cyano-4′-pentylparaterphenyl (5TB) [22] have been successfully applied in various displays, smart windows, and electronics equipment.

The successful application of LC requires two prerequisites. The first requisite is that the LC shows an appropriate phase temperature range and phase structure [23]. Generally,

the phase transitions of common rod-like LC molecules are controlled by thermal behavior. However, the development of modern advanced devices requires other ways to regulate the phase transition and phase, such as light, radiation, electricity, and so on [24,25]. These approaches require LC molecules to possess the specific structures needed to realize the process. The rod-like LC molecules containing azobenzene have been used for photo-controlling phase transition and phase behavior [26–28]. With the stimulation of light or heat, azobenzene proceeds the *trans-cis* isomerization [29,30], which leads to the accumulation of the *cis*-isomers and causes the phase transition from LC phase to isotropic phase. The second requirement is that the LC molecules are able to be easily oriented through an external field, such as force [31], electricity [32], and magnetism [33]. To date, homogeneous, homeotropic, twisted, splay, azimuthal, or radial alignments of LC molecules are successfully realized through mechanical rubbing, electric fields, and magnetic fields [34,35]. The resultant LC-oriented films with excellent optical and mechanical properties have also been applied in all kinds of optical devices [4,36,37]. Recently, photoalignment has become one of the most attractive methods since wavelength- and intensity-adjustable light allows for remote wireless control and accurate manipulation [38–41]. Similarly, the realization of photoalignment also requires a specific structure for the LC molecules. Fortunately, LC molecules with azobenzene can be easily oriented perpendicular to the polarized direction of ultraviolet (UV) light [42]. Thus, azobenzene has successfully become a popular and famous molecule in recent decades. Numerous azobenzene LC compounds with different architectures have been designed and synthesized, and their LC self-assembly behavior and the relationship between structure and property, have also been substantially investigated [43,44]. Meanwhile, a large amount of functional materials containing azobenzene, like LC elastomers (LCEs), LC polymer networks (LCNs), LC block copolymers, etc., have been obtained [45–47].

In our previous work, we successfully realized the alignment control of nematic LC using gold nanoparticles grafted by azobenzene LC polymer, but the synthesis of the nanoparticles is very difficult, which limits their further application [48]. Thus, we attempted to design a simple LC molecular and propose a versatile method to realize the alignment control of nematic LC. In this work, we prepared a novel long rod-like LC molecule containing double azobenzene (M1). The molecular structure is shown in Scheme 1. The chemical structure of the molecule has been confirmed by nuclear magnetic resonance (NMR) and Fourier transform infrared spectroscopy (FTIR). The phase structure and phase transition have been determined by polarizing optical microscopy (POM), differential scanning calorimetry (DSC), and one-dimensional wide-angle X-ray diffraction (1D WAXD). The resultant LC molecule presents an ultrahigh LC temperature range until decomposition, which can be potentially applied in special equipment. Further, the prepared LC compound M1 was incorporated as a dopant into 5CB with different concentrations. The LC temperature range of the obtained LC mixture can be freely regulated. Surprisingly, after doping a certain amount of M1, this kind of LC mixture can realize a spontaneous vertical orientation. Due to the presence of the *trans-cis* isomerization of azobenzene, the LC mixture can undergo a reversible transition between vertical and random orientation under the irradiation of both UV light and 470 nm visible light.

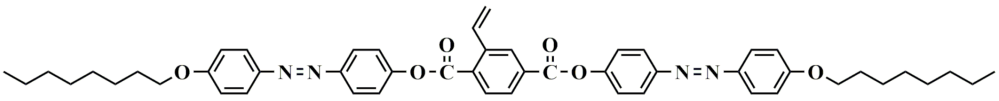

Scheme 1. Chemical structure of compound M1.

2. Experimental Section

Materials. 4-Acetamidophenol (98%), 4-cyano-4′-pentylbiphenyl (99%), 1-bromobutane (98%), 1-bromohexane (99%), 1-bromooctane (99%), 1-bromodecane (99%), and 1-bromododecane (98.5%) were purchased from Energy Chemical, Shanghai, China. Thionyl chloride (SOCl2) and triethylamine were obtained from Sinopharm Chemical Reagent Co.,

Ltd., Shanghai, China. Phenol was purchased from J&K Scientific Ltd., Beijing, China. 1,4-Benzenedicarboxylic acid was synthesized according to the literature.

Instruments and Measurements. A Bruker ARX400 spectrometer was used to carry out ^{1}H NMR experiments, where tetramethylsilane (TMS) and deuterated chloroform ($CDCl_3$) were the internal standard and the solvent, respectively. Fourier transform infrared spectroscopy (FTIR) spectra were recorded in KBr pellets on a PE Spectrum One FTIR spectrometer.

A differential scanning calorimetry (DSC) experiment was carried on the TA Q10 calorimeter with a programmed heating procedure in nitrogen. A polarized optical microscope (POM) experiment was performed on the Leica DM-LM-P polarizing optical microscope with a Mettler FP82HT heating stage. A one-dimensional wide-angle X-ray diffraction (1D WAXD) experiment was carried out on a Bruker D8 Discover powder diffractometer equipped with Anton Paar TCU 110 hot stage and an Anton Parr TCU-100 temperature control unit. The light stimulation was accomplished by a FUWO lamp, where the UV source is 365 nm (FUV-6BK 150 mW/cm^2) and the visible light source is 470 nm (F7B-B20 150 mW/cm^2).

Synthesis. The synthetic route of compound M1 is shown in Scheme 2. The detailed synthesis information is as follows.

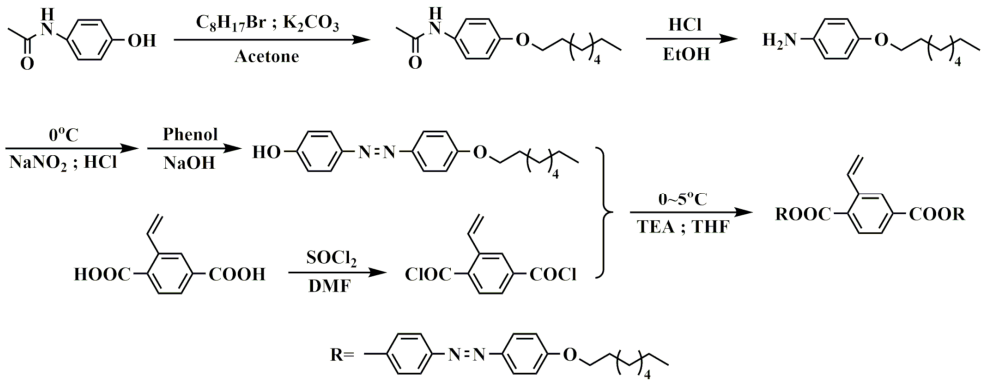

Scheme 2. Synthetic route of the compound M1.

Synthesis of 4-Octyoxyacetylbenzene. 4-Acetamidophenol (18.12 g, 0.12 mol), anhydrous potassium carbonate (33.09 g, 0.24 mol), 1-bromooctane (34.72 g, 0.18 mol), and 200 mL of acetone were mixed in a 500-mL round-bottom flask. The mixture was stirred and refluxed for 16 h at 65 °C. After the reaction was terminated, the mixture was immediately filtered. Subsequently, the solvent was removed by rotary evaporation. The solution was rinsed with hot water and petroleum ether several times. The crude product was placed in vacuum at 40 °C for 12 h. A white solid powder product was obtained. The yield was 90%.

^{1}H NMR($CDCl_3$-d6) δ (ppm): 7.31 (d, 2H, Ar-H), 7.06 (s, 1H, Ar-NH) 6.84 (d, 2H, Ar-H), 3.89 (t, 2H, -OCH_2-), 2.09 (t, 3H, -$COCH_3$), 1.32~1.73 (t, 12H, -CH_2-), 0.87 (t, 3H, -CH_3).

Synthesis of 4-n-Octyloxyaniline. 4-Octyoxyacetylbenzene (12.21 g, 0.05 mol) was dissolved in a mixture of 150 mL of anhydrous ethanol and 30 mL of hydrochloric acid (37%) in a 250-mL round-bottom flask. This mixture was stirred and refluxed at 80 °C for 48 h. After the reaction was terminated, the solution was cooled to room temperature. Then, the solution was put in 500 mL of ice water. A large amount of white precipitate was obtained. The pH of the mixture was adjusted to 7–8 with a certain amount of NaOH aqueous solution. Subsequently, this mixture was filtered. The obtained white solid powder was placed under vacuum at 40 °C for 12 h. The yield was 80%.

^{1}H NMR($CDCl_3$-d6) δ (ppm): 7.30 (d, 2H, ArH), 6.86 (d, 2H, Ar-H), 3.89 (t, 2H, -OCH_2-), 3.69–3.20 (s, 2H, -NH_2), 1.75–1.29 (m, 12H, -CH_2-), 0.88 (t, 3H, -CH_3).

Synthesis of 4-(4′-Hydroxy)octyloxyazobenzene. A mixture of 4-n-octyloxyaniline (10.00 g, 0.045 mol), deionized water (100 mL), and 37% hydrochloric acid (10 mL) were

added into a 250-mL round-bottom flask. Then, the flask was placed in an ice-water bath. Next, 45 mL of $NaNO_2$ aqueous solution (4.23 g, 0.06 mol) was added dropwise into the flask within 15 min under stirring. After an hour, a brownish red solution of diazonium salt was obtained. The obtained solution of diazonium salt was dropped into a 1000-mL beaker containing phenol (5.64 g, 0.06 mol) and 400 mL of deionized water under ice-water conditions within 15–20 min. During this process, the pH of the reactant was kept around 9–10 using 15 wt% NaOH aqueous solution. Then, the pH of the mixture was further adjusted to around 3–4 through adding 10 wt% hydrochloric acid after an hour reaction. Afterwards, the reactant mixture was filtered, and the obtained solid was rinsed with deionized water until a neutral state was obtained. Further, the mixed reagent with ethanol and deionized water (1:1) was used for recrystallization three times. The obtained crude product was placed under vacuum at 50 °C for 24 h. At last, the crude product was purified by column chromatography using the mixed solvent of dichloromethane and petroleum ether (3:1) as the developing agent. Orange flake crystals were obtained; the yield was 85%.

^{1}H NMR(DMSO-d6) δ (ppm): 10.16 (s, 1H, -OH), 7.81–7.74 (m, 4H, Ar-H), 7.01–6.92 (m, 4H, Ar-H), 4.06 (s, 2H, -OCH_2), 1.75 (s, 2H, -CH_2-), 1.44–1.33 (t, 6H, -CH_2-), 0.90 (t, 3H, -CH_3).

Synthesis of 1,4-Benzenedicarboxylic acid. 1,4-Benzenedicarboxylic acid was lab-made according to previous work [49].

^{1}H NMR (δ, ppm, DMSO-d_6): 8.26 (s, 1H, Ar-H), 7.91 (d, 2H, Ar-H), 6.68 (d, 2H, =CH-), 5.76 (d, 1H,=CH_2), 5.43 (d, 1H,=CH_2).

Synthesis of Bis(4-((4-(octyloxy)phenyl)diazenyl)phenyl)2-vinylterephthalate (M1). A mixture of 1,4-benzenedicarboxylic acid (1.00 g, 0.005 mol), $SOCl_2$ (30 mL), nitrobenzene (1 drop), and anhydrous tetrahydrofuran (THF) (2–3 drops) was added into a 100-mL round-bottom flask. The reaction was stirred at 60 °C until the solution became clear. Then, the solvent was removed by rotary evaporation. Next, 30 mL of anhydrous THF was added into the acyl chloride solution. Then. 4-(4′-hydroxy) octyloxyazobenzene (4.27 g, 0.013 mol), anhydrous THF (60 mL), and anhydrous triethylamine (3.53 g, 0.035 mol) were added into a 250-mL round-bottom flask. Next, the flask with the mixture was further stirred in an ice-water bath. The acyl chloride solution was added dropwise into the flask through a constant pressure funnel, then the reaction was maintained for 12 h at room temperature. The mixture was filtered under reduced pressure, and the solvent of the obtained solution was removed by rotary evaporation. The solid mixture was dissolved in the flask with chloroform. Then, the solution was rinsed with deionized water several times and dried overnight with anhydrous magnesium sulfate. Further, the solution was filtered, and the crude product was obtained by rotary evaporate. At last, the crude product was purified by column chromatography using dichloromethane as the developing agent. A golden powder product was obtained. The yield was 60%.

^{1}H NMR($CDCl_3$) δ (ppm): 8.50 (s, 1H, Ar-H), 8.26 (q, 2H, Ar-H), 8.01 (q, 4H, Ar-H), 7.95 (q, 4H, Ar-H), 7.60 (d, 1H, -CH=CH_2), 7.42 (q, 4H, Ar-H), 7.01 (m, 4H, Ar-H), 5.90 (d, 1H, -CH=CH_2), 5.53 (d, 1H, -CH=CH_2), 4.07 (m, 4H, -OCH_2-), 1.85 (m, 4H, -CH_2-), 1.49~1.29 (m, 20H, -CH_2-), 0.92 (t, 6H, -CH_3).

^{13}C-NMR($CDCl_3$) δ (ppm): 14.12 (-$\underline{C}H_3$), 22.68 (-$\underline{C}H_2$-), 26.04 (-$\underline{C}H_2$-), 29.22–29.37 (-$\underline{C}H_2$-), 31.84 (-$\underline{C}H_2$-), 68.44 (-$\underline{C}H_2$-O-), 114.78 (-CH=$\underline{C}H_2$), 122.20–124.91 (azobenzene C ortho to C-O), 128.79–134.60 (aromatic and =$\underline{C}$H-), 146.74–150.65(aromatic $\underline{C}$-N), 161.95 (C=O), 164.00–164.66 (C=O).

FTIR-KBr: -CH_3 (2952), -CH_2- (2937, 2854), -CO- (1740), -CH=CH_2 (1603), -C=C- (1603,1582,1493), -C-O-C- (1240, 1146, 1025).

Preparation of LC Cells. The glass slides were treated with piranha solution, which consisted of 30 mL of hydrogen peroxide and 70 mL of concentrated sulfuric acid at 130 °C for 30 min. Then, the slides were rinsed with deionized water five times. Further, two slides were used for preparing a LC cell separated by two strips of Mylar film as spacer, and were lastly fixed with two clips. The thickness of the LC cell was controlled by the Mylar film with a thickness of 2.5 μm.

3. Results and Discussion

Synthesis, Phase Behavior, and Phase Structure of M1. The compound M1 was successfully synthesized through multistep reactions according to Scheme 2, using 4-acetamidophenol and 1,4-benzenedicarboxylic acid as the raw materials. The chemical structures of M1 and intermediates were confirmed by ^{1}H NMR, ^{13}C NMR, and FTIR. The detailed information was described above in the experimental section. The phase transition behavior of compound M1 was determined by DSC. To erase the thermal history, 6 mg compound of M1 was first heated to 200 °C at a rate of 20 °C/min followed by isothermal annealing for 5 min. Then, the first cooling trace and the second heating trace were recorded at 10 °C/min. As shown in Figure 1, an obvious phase transition peak can be observed during both the heating and cooling process. To further explore the LC properties of compound M1, a POM experiment was carried out to investigate the LC texture. As shown in Figure 1b, the POM result reveals that compound M1 could show an obvious birefringence. In this experiment process, when the temperature was increased above the melting point (T_m), M1 showed a clear birefringence phenomenon, and the birefringence of the monomer still remained until the temperature rose towards its decomposition temperature, which demonstrated the wide range of LC phase of the compound M1, and its clearing point exceeded the decomposition temperature.

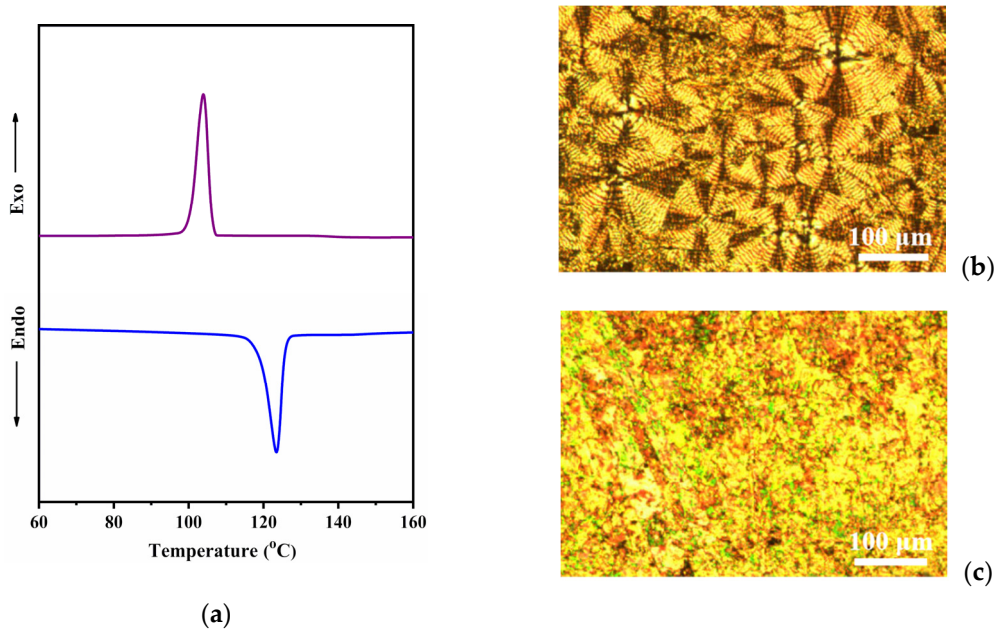

(**a**) (**b**) (**c**)

Figure 1. (**a**) Differential scanning calorimetry (DSC) thermogram of M1 at 10 °C/min during the first cooling process and the second heating process; polarized optical microscopy (POM) of the compound M1 at (**b**) 50 °C, (**c**) 150 °C during the heating (magnification: ×100).

Subsequently, the temperature-variable 1D-WAXD experiments were carried out to investigate the phase structure and LC properties. As shown in Figure 2, the distinct crystalline phase structure was observed below 110 °C. When the temperature was increased to 150 °C, the original peaks located in both low-angle and high-angle regions disappeared, which indicated that the crystal had melted. Meanwhile, two new peaks appeared in a low-angle region and a diffused amorphous broad halo was observed at approximately $2\theta = 20^{\circ}$ in the high-angle region, indicating that a low-ordered LC phase formed. Upon further analyzing the diffraction peaks, we found that the ratio of the diffraction vectors was 1:2, implying that compound M1 could form a smectic structure. Meanwhile, as the temperature was increased to 300 °C, the diffraction still remained, which meant that the compound M1 could present this smectic structure until decomposition. This phenomenon is rare in a LC system in addition to mesogen "jacket" liquid crystalline polymers [50].

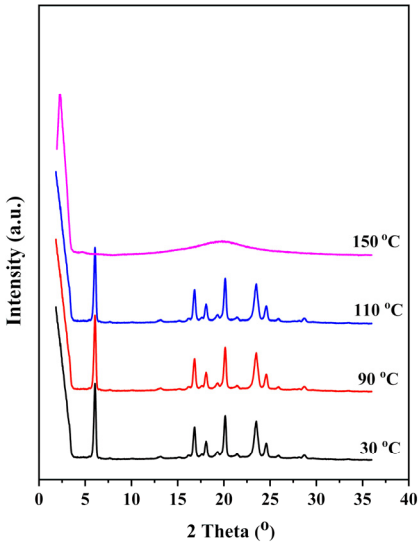

Figure 2. One-dimensional wide-angle X-ray diffraction (1D WAXD) pattens of M1 during heating process.

Nematic LC Range Regulation by Doping with M1. The above experimental results revealed that M1 showed a wide range of LC temperature from 150 °C to decomposition temperature. Further, this compound M1 was incorporated as a dopant into common commercialized LC materials to control the nematic LC range. For effective adjustment of the LC temperature, a series of 5CB/M1 mixtures with different doping concentrations were prepared using $CHCl_3$ as the solvent. The prepared samples with the mass fractions of 5CB with 20 wt%, 40 wt%, 60 wt%, 80 wt%, 90 wt%, 95 wt%, and 97.5 wt% were named as the sample 1, 2, 3, 4, 5, 6, and 7, respectively. The mixture was ultrasonic treated to ensure a completely dissolved and uniform mix, and then was naturally volatilized at room temperature. Figure 3 shows the mixture in solution and solid state after volatilization.

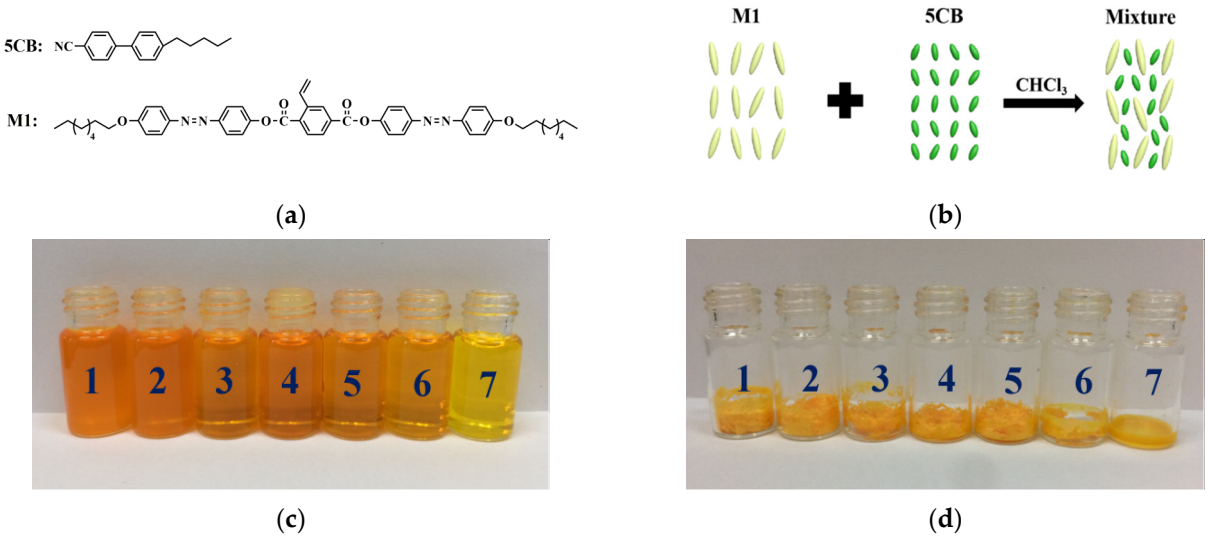

Figure 3. (**a**) Chemical structure of 5CB and M1. (**b**) Fabrication process of the M1 and 5CB liquid crystal (LC) mixtures. (**c**) In $CHCl_3$ solution and (**d**) evaporated solvent photographs of LC mixture samples (1–7) with different mass fractions of M1 and 5CB. The mass fractions of 5CB in samples (1–7) are 20 wt%, 40 wt%, 60 wt%, 80 wt%, 90 wt%, 95 wt%, and 97.5 wt%, respectively.

Herein, sample 7 was used as an example to elucidate phase behavior. Firstly, the LC cell was prepared through putting 1–3 mg of sample 7 into two sealed clean glass

slides. Then, POM was performed to investigate the LC behavior. Figure 4 shows the temperature-variable POM test results of sample 7. When the temperature was lower than 90 °C during the heating process, sample 7 exhibited a crystal structure. As the temperature increased to 90 °C, a smectic phase was gradually formed. Eventually, the isotropic phase was achieved at 134 °C. During the cooling process, it exhibited a similar experimental phenomenon at different temperatures. Furthermore, POM results exhibited a partial homeotropic orientation. Therefore, the hydrophilic substrates were used in the subsequent experiments to enhance the anchoring effect of M1 molecules to realize a better vertical orientation.

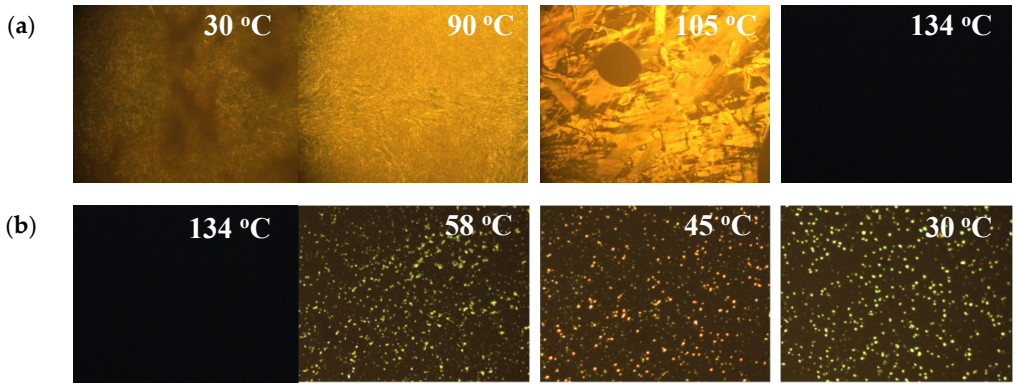

Figure 4. POM of sample 7 during heating (**a**) and cooling (**b**).

Furthermore, temperature-variable 1D WAXD was utilized to explore the LC properties and phase structures of the mixtures. The experimental result is shown in Figure 5a. The result indicated that sample 7 exhibited a crystal structure at room temperature. When the temperature was increased to 90 °C, it changed from a crystal phase to a LC phase. The results of other samples are shown in Figure S1; all samples showed an ordered structure of LC phase. The experimental results were in good agreement with the POM test results. Combing the results of the POM and temperature-variable 1D WAXD (Table 1), we concluded that doping with an appropriate M1 could effectively widen the LC temperature range of 5CB. The LC temperature ranges in the series of samples are summarized in Figure 5b. The result of 1D WAXD patterns showed both sharp diffractions in the low-angle and high-angle regions, which indicated that the mixture formed a smectic phase rather than a nematic phase.

Table 1. Phase transition temperature of M1 and 5CB LC mixtures.

Sample	0	1	2	3	4	5	6	7	8
5CB (wt%)	0	20	40	60	80	90	95	97.5	100
M1 (wt%)	100	80	60	40	20	10	5	2.5	0
T_{iso} (°C)	/	286	240	230	230	225	210	134	35
T_m (°C)	150	135	120	100	100	90	90	90	24

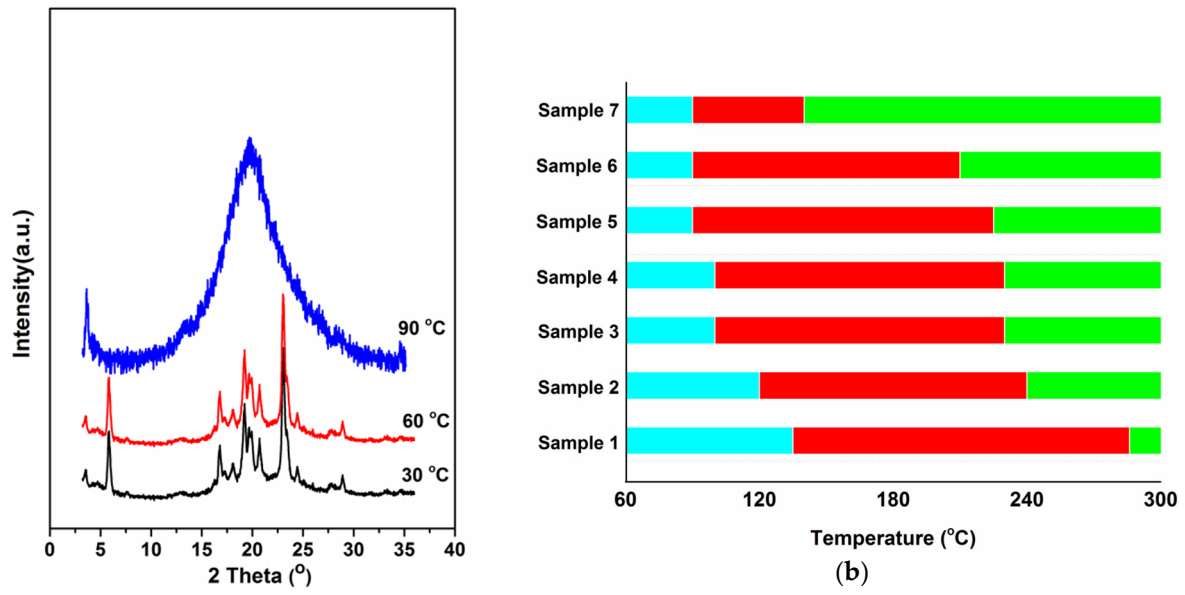

Figure 5. 1D WAXD patterns of sample 7 during heating process (**a**), and LC temperature range of samples 1–7 (**b**). Crystal phase (azure), smectic phase (red), and isotropic phase (green).

Alignment Behavior of 5CB Doping with M1. Due to the M1 molecule containing double long alkanes, we speculated that this molecule could present a strong anchoring effect with substrate, which could be used for orientating LC. Thus, the orientation behavior of the series of samples mentioned above was investigated. Firstly, the bare glass slides were treated with piranha solution to form a hydrophilic surface, and were further rinsed by deionized water several times. Two treated glass slides were used to prepare a LC cell. Subsequently, the sample was filled in the LC cell on a hot stage by capillary force. Figure 6 shows the images of the serial sample 1 to sample 7 under POM above T_m. All the images of different samples with different concentrations showed a dark field, which was different from the bright field for pure M1 and 5CB under orthoscopic POM. Meanwhile, the typical black crosses could be found under the conoscopic POM (the insets in Figure 6), indicating that all samples presented vertical alignment in the LC cells. Evidently, the homeotropic alignment of the commercial LC material 5CB could be realized through doping with some M1 molecules. Our previous work had demonstrated that homeotropic alignment of 5CB could be achieved by doping some Au@TE-PAzo nanoparticles due to the synergistic interaction of the internal gold core and the peripheral polymer ligand [51]. Notably, the deposition of Au@TE-PAzo NPs on the substrate through the interaction between the hydrophilic substrate and the gold core played a crucial role in the homeotropic alignment. In this work, we speculated that some of the dispersive M1 could be deposited on the substrate for the gravity effect. Therefore, the long alkane on both ends of the M1 could lead to a strong anchoring energy to induce the LC homeotropic alignment.

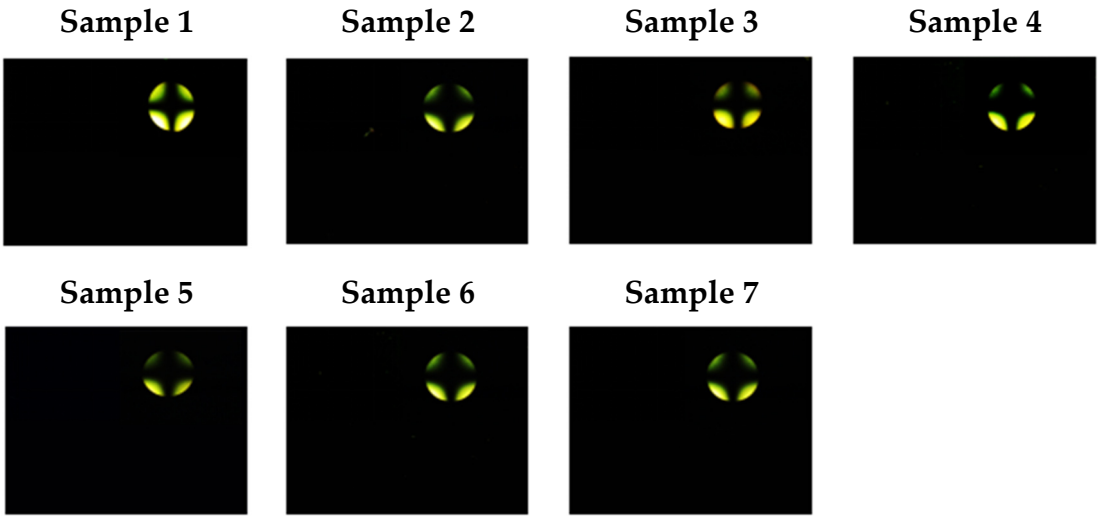

Figure 6. POM of the M1-doped 5CB mixtures with different mass fractions (insets are the conoscopic POM of the mixtures).

The photochemical behavior of the M1 in solution was investigated by UV-vis spectroscopy. Figure 7 shows the intensity variation of the absorption peak. The intensity of the peak located at 355 nm gradually decreased under the irradiation of 365 nm UV light, but the intensity of the peak located at 450 nm slightly increased. Further irradiating by visible light, the intensity of the two absorption peaks presented reversible transition, which was attributed to the typical *trans-cis* transformation of the azobenzene group. Meanwhile, this *trans-cis* transition of M1 gave an opportunity to regulate LC alignment through light irradiation.

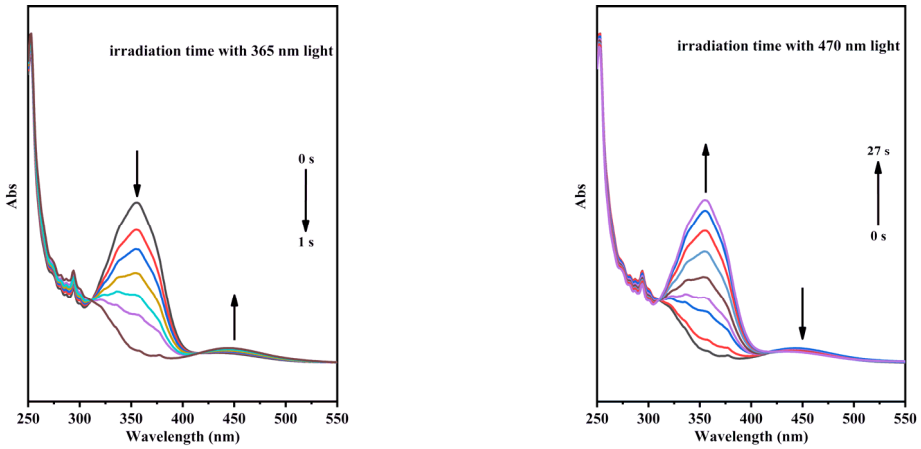

(**a**) (**b**)

Figure 7. M1 in $CHCl_3$ solution upon irradiation with UV light (**a**) and visible light (**b**).

Thus, light-regulating LC alignments were further investigated by UV and 470 nm visible light irradiation. Figure 8 shows POM images of the samples 1–7 irradiated by 365 nm and 470 nm light for different times. It was clearly observed that all the samples irradiated with a 365 nm ultraviolet light presented distinct birefringence phenomenon under orthoscopic POM. Meanwhile, the bright field could be observed under the conoscopic POM. Subsequently, when the samples were irradiated by 470 nm visible light, the birefringence phenomenon disappeared under orthoscopic POM, while the orthogonal black cross reappeared under the conoscopic POM, indicating the restoration of vertical alignment of the LC molecules. Evidently, the experimental results revealed that the vertical alignment of the mixtures could be regulated by UV and visible light irradiation.

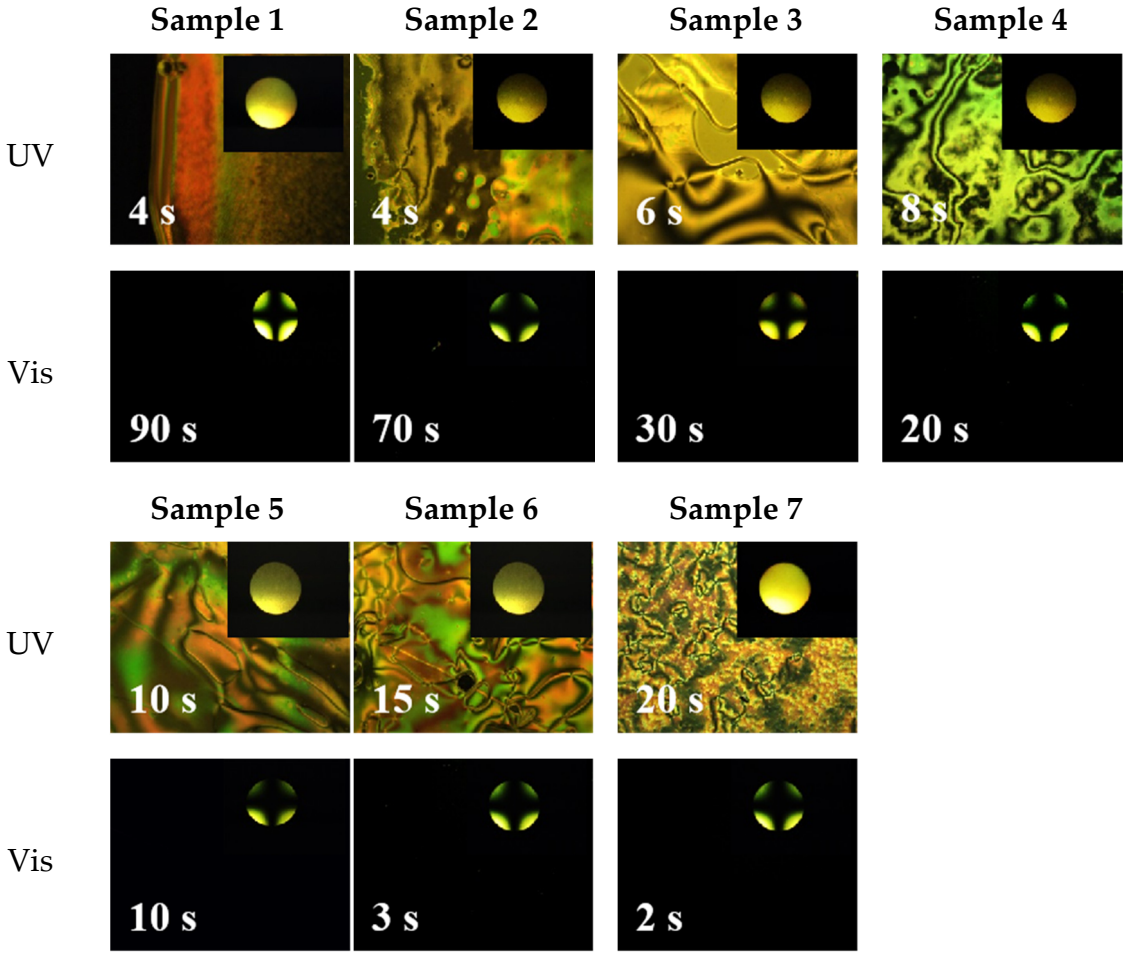

Figure 8. POM of the M1-doped 5CB mixtures with different mass fractions irradiated by 365 nm and 470 nm light for different times.

The results revealed that all samples could realize the transformation of LC orientation under the illumination of the UV and 470 nm visible light. It was especially notable that under the illumination of the UV light, the LC behavior did not disappear (even for sample 1, which contained 80% M1), which was different from the previous LCs containing azobenzene groups, whose LC structure was destroyed under UV light illumination [52]. This phenomenon may come from the long molecular length of M1. The mismatched dimensions between the M1 and 5CB lead to the stable existence of the nematic phase. Figure 9 describes the possible mechanisms for the above phenomenon. When the LC mixture was located in the LC cells, some M1 molecules contacted with the substrate first displayed a homeotropic orientation on account of the anchoring effect. Subsequently, the long molecular structure of M1 drove the whole LC mixture to present a homeotropic alignment. When the mixture was exposed to the irradiation of 365 nm light, the azobenzene mesogen in the mixture transferred from *trans* to *cis* conformation, which led to the disappearance of the regular vertical alignment. However, the large dimension in the *trans-cis* isomerism did not destroy the LC phase. Due to the experimental limitations, the variation of the LC phase during the illumination process was not observed, which needs to be further investigated in future work.

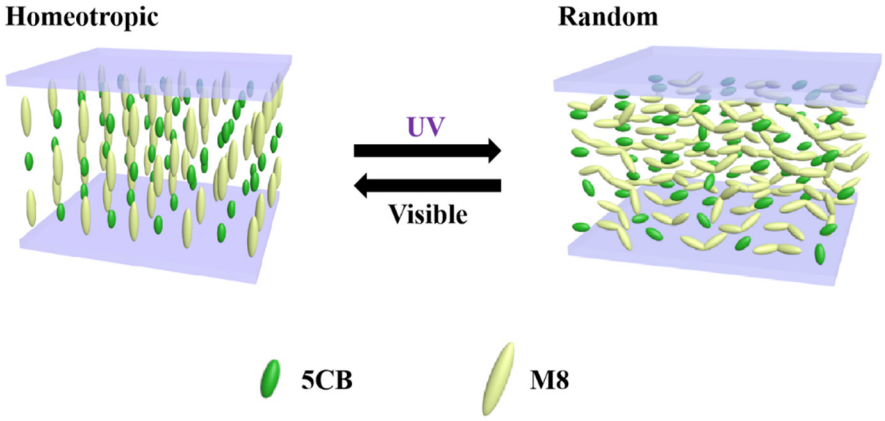

Figure 9. Illustration of the mechanisms of homeotropic and planar alignments.

4. Conclusions

In summary, we successfully synthesized a novel long rod-like LC molecule containing double azobenzene (M1). The chemical structure of the molecule was confirmed by ^{1}H NMR, ^{13}C NMR, and FTIR. The POM, DSC, and 1D WAXD experimental results showed that M1 exhibited a stable smectic structure even at ultrahigh temperature, which indicated that M1 presented a wide range of LC temperatures. Further, a series of samples constituted by different contents 5CB and M1 were prepared. Due to the content variation, this series of samples presented different LC temperature ranges. Meanwhile, the series of samples could present spontaneous vertical orientation on the hydrophilic glass substrate. When the LC cells were alternately exposed to UV irradiation and visible light, a reversible transition between homeotropic to random orientation of the LC molecules was realized due to the existence of azobenzene in compound M1. This work implied that this azobenzene LC and its mixtures with 5CB could have potential applications, especially in display and optical storage technologies.

Supplementary Materials: The following are available online at https://www.mdpi.com/article/10.3390/cryst11040418/s1, Figure S1: 1D WAXD pattems of samples(1, 2, 3, 4, 5, 6) during heating process.

Author Contributions: Conceptualization, Q.W. and H.C.; methodology, H.C.; software, H.X.; validation, Q.W., Y.D. and Z.-W.L.; formal analysis, Q.W.; investigation, H.C.; resources, H.C.; data curation, H.X.; writing—original draft preparation, H.C.; writing—review and editing, Q.W.; visualization, Q.W. and Z.-W.L.; supervision, H.-L.X.; project administration, H.-L.X.; funding acquisition, H.-L.X. All authors have read and agreed to the published version of the manuscript.

Funding: This research was funded by National Natural Science Foundation of China (NNSFC 21975215 and 21674088), the Scientific Research Foundation of Hunan Provincial Education Department (19A486), and the Hunan 2011 Collaborative Innovation Center of Chemical Engineering & Technology with Environmental Benignity and Effective Resource Utilization.

Conflicts of Interest: The authors declare no conflict of interest.

References

1. Bisoyi, H.K.; Bunning, T.J.; Li, Q. Stimuli-Driven Control of the Helical Axis of Self-Organized Soft Helical Superstructures. *Adv. Mater.* **2018**, *30*, 1706512. [CrossRef]
2. Bisoyi, H.K.; Li, Q. Light-Driven Liquid Crystalline Materials: From Photo-Induced Phase Transitions and Property Modulations to Applications. *Chem. Rev.* **2016**, *116*, 15089–15166. [CrossRef]
3. Cha, Y.J.; Gim, M.-J.; Oh, K.; Yoon, D.K. In-Plane Switching Mode for Liquid Crystal Displays Using a DNA Alignment Layer. *ACS Appl. Mater. Interface* **2015**, *7*, 13627–13632. [CrossRef]
4. Fernández, R.; Gallego, S.; Márquez, A.; Francés, J.; Martínez, F.J.; Pascual, I.; Beléndez, A. Analysis of holographic polymer-dispersed liquid crystals (HPDLCs) for tunable low frequency diffractive optical elements recording. *Opt. Mater.* **2018**, *76*, 295–301. [CrossRef]
5. Kendhale, A.M.; Schenning, A.P.H.J.; Debije, M.G. Superior alignment of multi-chromophoric perylenebisimides in nematic liquid crystals and their application in switchable optical waveguides. *J. Mater. Chem. A* **2013**, *1*, 229–232. [CrossRef]

6. Rushnova, I.I.; Melnikova, E.A.; Tolstik, A.L.; Muravsky, A.A. Electrically switchable photonic liquid crystal devices for routing of a polarized light wave. *Opt. Commun.* **2018**, *413*, 179–183. [CrossRef]
7. Kostko, A.F.; Cipriano, B.H.; Pinchuk, O.A.; Ziserman, L.; Anisimov, M.A.; Danino, D.; Raghavan, S.R. Salt Effects on the Phase Behavior, Structure, and Rheology of Chromonic Liquid Crystals. *J. Phys. Chem. B* **2005**, *109*, 19126–19133. [CrossRef]
8. Jayaraman, A.; Schweizer, K.S. Effective Interactions, Structure, and Phase Behavior of Lightly Tethered Nanoparticles in Polymer Melts. *Macromolecules* **2008**, *41*, 9430–9438. [CrossRef]
9. Jiang, R.; Jin, Q.; Li, B.; Ding, D.; Wickham, R.A.; Shi, A.-C. Phase Behavior of Gradient Copolymers. *Macromolecules* **2008**, *41*, 5457–5465. [CrossRef]
10. Jiao-jiao, Y.; Yao-jian, F.; Lei, T.; He-lou, X.; Hai-liang, Z. Phase Behavior and Phase Structure of Polymerized Ionic Liquid Crystals with Different Alkyl Tail Length Based on Jacketing Effect. *Acta Polym. Sin.* **2017**, *10*, 1616–1623.
11. Herrmann-Schönherr, O.; Wendorff, J.H.; Ringsdorf, H.; Tschirner, P. Structure of an aromatic polyamide with disc-like mesogens in the main chain. *Die Makromol. Chem. Rapid Commun.* **1986**, *7*, 791–796. [CrossRef]
12. Nguyen, H.T.; Sigaud, G.; Achard, M.F.; Hardouin, F.; Twieg, R.J.; Betterton, K. Rod-like mesogens with antipathetic fluorocarbon and hydrocarbon tails. *Liq. Cryst.* **1991**, *10*, 389–396. [CrossRef]
13. Okano, K.; Mikami, Y.; Yamashita, T. Liquid-Crystalline Polymer with a Block Mesogenic Side Group: Photoinduced Manipulation of Nanophase-Separated Structures. *Adv. Funct. Mater.* **2009**, *19*, 3804–3808. [CrossRef]
14. Sekine, T.; Niori, T.; Sone, M.; Watanabe, J.; Choi, S.-W.; Takanishi, Y.; Takezoe, H. Origin of Helix in Achiral Banana-Shaped Molecular Systems. *Jpn. J. Appl. Phys.* **1997**, *36*, 6455–6463. [CrossRef]
15. Weissflog, W.; Demus, D.; Diele, S.; Nitschke, P.; Wedler, W. From laterally branched mesogens to novel twin molecules. *Liq. Cryst.* **1989**, *5*, 111–122. [CrossRef]
16. Guillevic, M.-A.; Bruce, D.W. Mesomorphic imines and their complexes with rhenium (I): A cubic mesophase in a rod-like mesogen with perfluorinated terminal chains. *Liq. Cryst.* **2000**, *27*, 153–156. [CrossRef]
17. Lee, M.; Yoo, Y.-S. Supramolecular organization of block oligomers based on rod-shaped mesogen into liquid crystalline assembly. *J. Mater. Chem.* **2002**, *12*, 2161–2168. [CrossRef]
18. Zheng, J.-F.; Yu, Z.-Q.; Liu, X.; Chen, X.-F.; Yang, S.; Chen, E.-Q. Side-chain liquid-crystalline polymers based on flexible rod-like mesogen directly attached to backbone. *J. Polym. Sci. Part A Polym. Chem.* **2012**, *50*, 5023–5031. [CrossRef]
19. Tripathi, C.S.P.; Losada-Pérez, P.; Glorieux, C.; Kohlmeier, A.; Tamba, M.-G.; Mehl, G.H.; Leys, J. Nematic-nematic phase transition in the liquid crystal dimer CBC9CB and its mixtures with 5CB: A high-resolution adiabatic scanning calorimetric study. *Phys. Rev. E* **2011**, *84*, 041707. [CrossRef]
20. Marinov, Y.G.; Hadjichristov, G.B.; Petrov, A.G.; Prasad, S.K. Thin films of silica nanoparticle doped nematic liquid crystal 7CB for electro-optic modulation. *Photonics Lett. Pol.* **2015**, *7*, 94–96.
21. Jayaprada, P.; Rao, M.; Pardhasaradhi, P.; Prasad, P.D.; Manepalli, R.; Pisipati, V. Optical studies of n-octyloxy-cyanobiphenyl (8ocb) with dispersed ZnO nanoparticles for display device application. *Optik* **2019**, *185*, 1226–1237. [CrossRef]
22. Singh, L.P.; Singh, N.P.; Srivastava, S.K. Terbium doped SnO_2 nanoparticles as white emitters and SnO_2: 5Tb/Fe_3O_4 magnetic luminescent nanohybrids for hyperthermia application and biocompatibility with HeLa cancer cells. *Dalton Trans.* **2015**, *44*, 6457–6465. [CrossRef] [PubMed]
23. Wu, Z.; Ji, C.; Zhao, X.; Han, Y.; Müllen, K.; Pan, K.; Yin, M. Green-Light-Triggered Phase Transition of Azobenzene Derivatives toward Reversible Adhesives. *J. Am. Chem. Soc.* **2019**, *141*, 7385–7390. [CrossRef]
24. Yao, Y.; Waters, J.T.; Shneidman, A.V.; Cui, J.; Wang, X.; Mandsberg, N.K.; Li, S.; Balazs, A.C.; Aizenberg, J. Multiresponsive polymeric microstructures with encoded predetermined and self-regulated deformability. *Proc. Natl. Acad. Sci. USA* **2018**, *115*, 12950–12955. [CrossRef]
25. Lehmann, W.; Skupin, H.; Tolksdorf, C.; Gebhard, E.; Zentel, R.; Krüger, P.; Lösche, M.; Kremer, F. Giant lateral electrostriction in ferroelectric liquid-crystalline elastomers. *Nature* **2001**, *410*, 447–450. [CrossRef] [PubMed]
26. Lu, X.; Guo, S.; Tong, X.; Xia, H.; Zhao, Y. Tunable Photocontrolled Motions Using Stored Strain Energy in Malleable Azobenzene Liquid Crystalline Polymer Actuators. *Adv. Mater.* **2017**, *29*, 1606467. [CrossRef]
27. Mahimwalla, Z.; Yager, K.G.; Mamiya, J.-I.; Shishido, A.; Priimagi, A.; Barrett, C.J. Azobenzene photomechanics: Prospects and potential applications. *Polym. Bull.* **2012**, *69*, 967–1006. [CrossRef]
28. Ni, B.; Xie, H.-L.; Tang, J.; Zhang, H.-L.; Chen, E.-Q. A self-healing photoinduced-deformable material fabricated by liquid crystalline elastomers using multivalent hydrogen bonds as cross-linkers. *Chem. Commun.* **2016**, *52*, 10257–10260. [CrossRef] [PubMed]
29. Zhou, H.; Xue, C.; Weis, P.; Suzuki, Y.; Huang, S.; Koynov, K.; Auernhammer, G.K.; Berger, R.; Butt, H.-J.; Wu, S. Photoswitching of glass transition temperatures of azobenzene-containing polymers induces reversible solid-to-liquid transitions. *Nat. Chem.* **2017**, *9*, 145–151. [CrossRef] [PubMed]
30. Ichimura, K. Photoalignment of Liquid-Crystal Systems. *Chem. Rev.* **2000**, *100*, 1847–1874. [CrossRef]
31. Lu, H.-F.; Wang, M.; Chen, X.-M.; Lin, B.-P.; Yang, H. Interpenetrating liquid-crystal polyurethane/polyacrylate elastomer with ultrastrong mechanical property. *J. Am. Chem. Soc.* **2019**, *141*, 14364–14369. [CrossRef] [PubMed]
32. Urayama, K.; Honda, S.; Takigawa, T. Deformation Coupled to Director Rotation in Swollen Nematic Elastomers under Electric Fields. *Macromolecules* **2006**, *39*, 1943–1949. [CrossRef]

33. Schuhladen, S.; Preller, F.; Rix, R.; Petsch, S.; Zentel, R.; Zappe, H. Iris-Like Tunable Aperture Employing Liquid-Crystal Elastomers. *Adv. Mater.* **2014**, *26*, 7247–7251. [CrossRef] [PubMed]
34. Ito, N.; Sakamoto, K.; Arafune, R.; Ushioda, S. Relation between the molecular orientations of a very thin liquid crystal layer and an underlying rubbed polyimide film. *J. Appl. Phys.* **2000**, *88*, 3235–3241. [CrossRef]
35. Van der Vegt, N.F.A.; Müller-Plathe, F.; Geleßus, A.; Johannsmann, D. Orientation of liquid crystal monolayers on polyimide alignment layers: A molecular dynamics simulation study. *J. Chem. Phys.* **2001**, *115*, 9935–9946. [CrossRef]
36. Liang, X.; Chen, M.; Wang, Q.; Guo, S.; Zhang, L.; Yang, H. Active and passive modulation of solar light transmittance in a hybrid thermochromic soft-matter system for energy-saving smart window applications. *J. Mater. Chem. C* **2018**, *6*, 7054–7062. [CrossRef]
37. Liang, X.; Guo, C.; Chen, M.; Guo, S.; Zhang, L.; Li, F.; Guo, S.; Yang, H. A roll-to-roll process for multi-responsive soft-matter composite films containing Cs x WO 3 nanorods for energy-efficient smart window applications. *Nanoscale Horiz.* **2017**, *2*, 319–325. [CrossRef]
38. Pan, S.; Ho, J.Y.; Chigrinov, V.G.; Kwok, H.S. Novel Photoalignment Method Based on Low-Molecular-Weight Azobenzene Dyes and Its Application for High-Dichroic-Ratio Polarizers. *ACS Appl. Mater. Interfaces* **2018**, *10*, 9032–9037. [CrossRef]
39. Wang, L.; Li, Q. Photochromism into nanosystems: Towards lighting up the future nanoworld. *Chem. Soc. Rev.* **2018**, *47*, 1044–1097. [CrossRef]
40. Zheng, Z.-G.; Yuan, C.-L.; Hu, W.; Bisoyi, H.K.; Tang, M.-J.; Liu, Z.; Sun, P.-Z.; Yang, W.-Q.; Wang, X.-Q.; Shen, D.; et al. Light-Patterned Crystallographic Direction of a Self-Organized 3D Soft Photonic Crystal. *Adv. Mater.* **2017**, *29*, 1703165. [CrossRef] [PubMed]
41. Fukuhara, K.; Nagano, S.; Hara, M.; Seki, T. Free-surface molecular command systems for photoalignment of liquid crystalline materials. *Nat. Commun.* **2014**, *5*, 1–8. [CrossRef]
42. Matsumori, M.; Takahashi, A.; Tomioka, Y.; Hikima, T.; Takata, M.; Kajitani, T.; Fukushima, T. Photoalignment of an Azobenzene-Based Chromonic Liquid Crystal Dispersed in Triacetyl Cellulose: Single-Layer Alignment Films with an Exceptionally High Order Parameter. *ACS Appl. Mater. Interfaces* **2015**, *7*, 11074–11078. [CrossRef] [PubMed]
43. Luo, Z.-W.; Tao, L.; Zhong, C.-L.; Li, Z.-X.; Lan, K.; Feng, Y.; Wang, P.; Xie, H.-L. High-Efficiency Circularly Polarized Luminescence from Chiral Luminescent Liquid Crystalline Polymers with Aggregation-Induced Emission Properties. *Macromolecules* **2020**, *53*, 9758–9768. [CrossRef]
44. Zhang, P.; Kragt, A.J.J.; Schenning, A.P.H.J.; de Haan, L.T.; Zhou, G. An easily coatable temperature responsive cholesteric liquid crystal oligomer for making structural colour patterns. *J. Mater. Chem. C* **2018**, *6*, 7184–7187. [CrossRef]
45. Donovan, B.R.; Matavulj, V.M.; Ahn, S.k.; Guin, T.; White, T.J. All-Optical Control of Shape. *Adv. Mater.* **2019**, *31*, 1805750. [CrossRef] [PubMed]
46. Gelebart, A.H.; Mulder, D.J.; Vantomme, G.; Schenning, A.P.H.J.; Broer, D.J. A Rewritable, Reprogrammable, Dual Light-Responsive Polymer Actuator. *Angew. Chem. Int. Edit.* **2017**, *56*, 13436–13439. [CrossRef] [PubMed]
47. Liu, Y.; Xu, B.; Sun, S.; Wei, J.; Wu, L.; Yu, Y. Humidity- and Photo-Induced Mechanical Actuation of Cross-Linked Liquid Crystal Polymers. *Adv. Mater.* **2017**, *29*, 1604792. [CrossRef] [PubMed]
48. Kuang, Z.-Y.; Fan, Y.-J.; Tao, L.; Li, M.-L.; Zhao, N.; Wang, P.; Chen, E.-Q.; Fan, F.; Xie, H.-L. Alignment Control of Nematic Liquid Crystal using Gold Nanoparticles Grafted by the Liquid Crystalline Polymer with Azobenzene Mesogens as the Side Chains. *ACS Appl. Mater. Interfaces* **2018**, *10*, 27269–27277. [CrossRef] [PubMed]
49. Zhang, D.; Liu, Y.-X.; Wan, X.-H.; Zhou, Q.-F. Synthesis and characterization of a new series of "mesogen-jacketed liquid crystal polymers" based on the newly synthesized vinylterephthalic acid. *Macromolecules* **1999**, *32*, 5183–5185. [CrossRef]
50. Zhu, J.-C.; Han, T.; Guo, Y.; Wang, P.; Xie, H.-L.; Meng, Z.G.; Yu, Z.-Q.; Tang, B.Z. Design and Synthesis of Luminescent Liquid Crystalline Polymers with "Jacketing" Effect andLuminescent Patterning Applications. *Macromolecules* **2019**, *52*, 3668–3679. [CrossRef]
51. Qi, H.; Hegmann, T. Multiple Alignment Modes for Nematic Liquid Crystals Doped with Alkylthiol-Capped Gold Nanoparticles. *ACS Appl. Mater. Interfaces* **2009**, *1*, 1731–1738. [CrossRef] [PubMed]
52. Ikeda, T.; Nakano, M.; Yu, Y.; Tsutsumi, O.; Kanazawa, A. Anisotropic Bending and Unbending Behavior of Azobenzene Liquid-Crystalline Gels by Light Exposure. *Adv. Mater.* **2003**, *15*, 201–205. [CrossRef]